Journal of Photochemistry and Photobiology A: Chemistry 199 (2008) 50–56

Contents lists available at ScienceDirect

Journal of Photochemistry and Photobiology A: Chemistry

journal homepage: www.elsevier.com/locate/jphotochem

Molecular assembly and photophysical properties of covalently bonded rare earth polymeric hybrid materials phen–RE–MSMA (MS)

Bing Yan*, Li-min Zhao, Jin-liang Liu

Department of Chemistry, Tongji University, Siping Road 1239, Shanghai 200092, China

ARTICLE INFO

Article history:
Received 10 December 2007
Received in revised form 26 March 2008
Accepted 24 April 2008
Available online 4 May 2008

Keywords:
Photophysical property
Inorganic/polymeric hybrid material
Rare earth ion
Covalently bonded

ABSTRACT

A new series of quaternary and ternary polymeric hybrid materials were assembled from 3-methacryloxypropyltrimethoxysilane (MS), methacrylic acid (MA), 1,10-phenanthroline (phen) and rare earth (Eu^{3+}, Tb^{3+}, and Dy^{3+}) precursors. MS and MSMA (copolymer of MS and MA) behave as structural functional component to form the inorganic polymeric network or inorganic/organic polymeric host through the coordination to rare earth ions, while phen acts as the energy sensitizer for the luminescence of rare earth ions. Subsequently, six novel hybrid materials (phen–Eu(Tb, Dy)–MS, phen–Eu(Tb, Dy)–MSMA) were obtained, in which inorganic component is connected with polymer component through covalent bond. It was found that the introduction of organic polymer unit has influence on the microstructure and especially the luminescent properties of hybrid materials. The quantum efficiency of Eu hybrids was also studied. All these hybrids exhibit the characteristic luminescence of rare earth ions, which substantiates optimum energy match and effective intramolecular energy transfer between the triplet state energy of phen and emissive energy level of Eu^{3+}, Tb^{3+} and Dy^{3+}. It was worth pointing out that the quaternary hybrid materials (phen–Eu^{3+}(Tb^{3+}, Dy^{3+})–MSMA) with organic polymer unit (MA) present stronger luminescence intensities, longer lifetimes than those of ternary ones without MA (phen–Eu^{3+}(Tb^{3+}, Dy^{3+})–MS), suggesting the introduction of organic chain (MA) is beneficial for the photophysical property of hybrids.

1. Introduction

Lanthanide complexes within various hosts make attractive materials for optical applications owing to their excellent luminescence characteristics from the electronic transitions between the 4f energy levels. The light-emission characteristics of lanthanide complex of phenanthroline were first described in 1960s. Since then, numerous compounds of lanthanide ions, in particular Eu^{3+} and Tb^{3+}, with various organic ligands, have been made and their crystal structures and luminescence behavior have been studied in detail. These complexes act as antennae of short wavelength radiation and, by energy transfer from the light-absorbing ligand to the lanthanide emission center, and they convert light to longer wavelengths, providing shifts greater than stokes shifts [1–8]. For this reason, lanthanide complexes may be of use in several applications, such as light concentrators for photovoltaic devices, labels for biological systems, and functional membranes and high-yield luminescent materials. So far, these complexes have been excluded from practical use as tunable solid-state lasers or phosphor devices because of their poor thermal stability and mechanical properties [9–11].

Several techniques have been developed to resolve these problems. In recent years, rare earth ions-containing polymers have attracted much attention for their potential application for the luminescence devices, laser systems and optical communication components [12–14]. The main reason is that polymer-based rare earth luminescent materials can be processed easily, which is the advantage in the fabrication of optical devices. These hybrid materials are classified in two categories from the viewpoints of domain sizes and chemical bonding. Organic–inorganic microcomposites are prepared by physical mixing of micrometer-sized organic and inorganic components. On the other hand, polymer hybrids are characterized by the formation of chemical bonds between organic and inorganic components to establish a mixing of organic and inorganic polymers at the molecular level [15–19]. Recently, some papers were reported on the luminescence behavior of Eu^{3+} and Tb^{3+} complexes with β-diketones, aromatic carboxylic acids and heterocylic ligands in polymer matrix [20–24]. Unfortunately, rare earth complexes were integrated into polymer matrix with weak interactions (van der Waals force or weak static effects) in these

* Corresponding author. Tel.: +86 21 65984663; fax: +86 21 65982287.
E-mail address: byan@tongji.edu.cn (B. Yan).

1010-6030/$ – see front matter © 2008 Elsevier B.V. All rights reserved.
doi:10.1016/j.jphotochem.2008.04.016

materials and it is not easy to obtain uniform material, which is possible to cause concentration quenching that restricts its practical application.

3-Methacryloxypropyltrimethoxysilane (MS) has been expected to be a good precursor for polymer hybrids because it has both methacrylate and trimethoxysilyl groups in a molecule. Babonneau and co-workers reported that hydrolytic polycondensation of MS provides linear oligomer [25]. Ishida and co-workers reported that the reaction under neutral or basic conditions results in the formation of rubber-like solids or insoluble precipitates [26]. Our research team presently did extensive work in the preparation of molecular hybrids with functional bridge connecting both siliceous backbone and aromatic carboxylic acids [27–32].

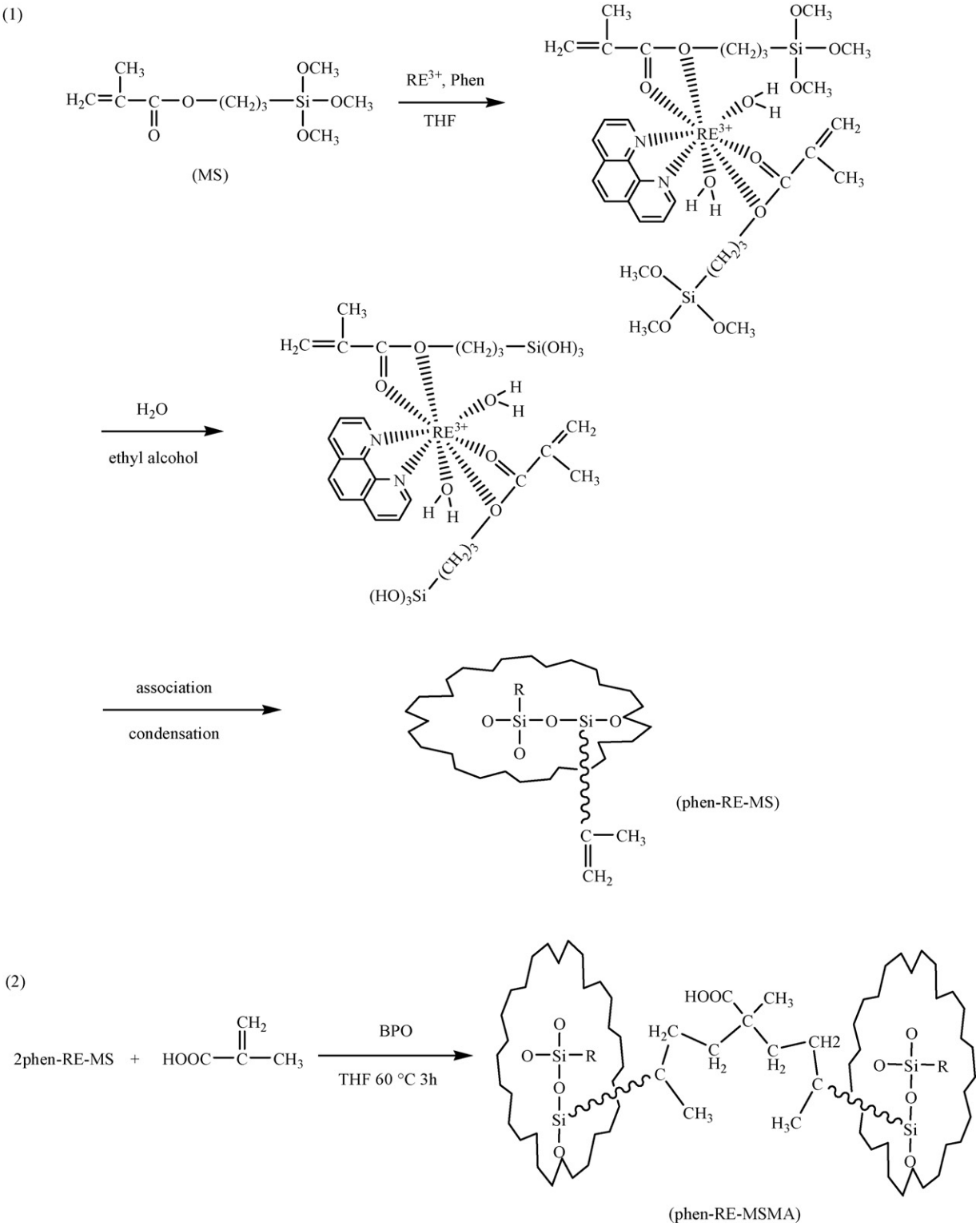

Fig. 1. Scheme of the synthesis process of polymer–inorganic hybrid materials.

In this work, MS was first connected with Eu^{3+} and Tb^{3+} by covalent bond and 1,10-phenanthroline (phen) was the coordinated ligand for obtaining better luminescence character. Then methacrylic acid (MA) was added in the polymerization process. Therefore, the polymer–Eu(Tb)–silicon hybrid material in which rare earth ions component connected with polymer component by the covalent bonds was prepared. The chemical structures, morphology and optical properties of hybrid material were examined. The hybrid material systems can be expected to have potential applications in photophysical sensors.

2. Experimental

MS was supplied by shanghai YaoHua chemical plant. 1,10-Phenanthroline, MA was purchased from shanghai chemical plant. Other starting reagents were used as received and were purified according to the usual method.

Phen, 3-(trimethoxysilyl)propyl methacrylate (MS), and terbium nitrate were dissolved into THF solution. The molar ratio of $RE(NO_3)_3{\cdot}6H_2O$ (RE = Eu, Tb and Dy)/MS/phen was 1:2:1, and the pH value was adjusted to be about 7.0. After stirring the solution for about 1 h, the reaction mixture with de-ionized water and ethyl alcohol were poured into a three-necked reactor to proceed the hydrolysis/condensation reaction. The reaction temperature was maintained at 333 K and the solution was stirred under a nitrogen flow for 2 h to obtain the colloidal MS–silica solution with RE^{3+} complexes. Then it was aged at 80 °C until the onset of gelation, which occurred within 5 days. Gels of ternary hybrid materials phen–RE–MS were collected as transparent monolithic bulks and ground as powder materials for the photophysical studies (see Fig. 1).

The colloidal phen–RE–MS obtained in the above was subsequently mixed with a homogeneous THF solution of the MA and the initiator, BPO, to proceed the polymerization reaction under nitrogen purging. MA was added with the molar ratio 1:2 to MS and BPO was about 0.003 g. The reaction temperature was maintained at 333 K for about 3 h. The coating liquid was concentrated under room temperature to remove the solvent THF using a rotary vacuum evaporator, then the thermal treatment was performed at 60 °C until the sample solidified. The poly-hybrid material prepared was denoted as phen–RE–MSMA (MSMA is MS and MA). A typical procedure for the preparation was according to reaction scheme in Fig. 1.

3. Physical measurements

Infrared spectroscopy were obtained in KBr pellets and recorded on a Nexus 912 AO446 FTIR spectrophotometer in the range of 4000–400 cm^{-1}. Ultraviolet absorption spectrum was measured with Agilent 8453 spectrophotometer. The fluorescence (excitation and emission) spectra were determined with PerkinElmer LS-55 spectrophotometer: excitation slit width = 10 nm and emission slit width = 5 nm. Low temperature phosphorescence spectrum was measured using the above instrument at 77 K. Luminescent lifetimes for hybrid materials were obtained with an Edinburgh Instruments FLS 920 phosphorimeter using a 450 W xenon lamp as excitation source (pulse width, 3 μs). The microstructure was characterized with scanning electronic microscope (SEM, Philps XL-30).

4. Results and discussion

The schematic diagram in Fig. 1 summarizes the reactions between the MA and terbium complex. First, MS and phen coordinated with Eu^{3+} in THF solution. No water was involved in the coordination process to prevent precursors hydrolyzing and influencing on the co-condensation. Then de-ionized water was added to accelerate the hydrolysis of the terminal silanol groups of MS and formed colloidal MSMA–silica, resulting in the ternary covalently bonded hybrid materials phen–RE–MS. In the step 2, MA for the crosslinking reagent was used for the preparation of final quaternary covalently bonded hybrid materials phen–RE–MSMA.

Fig. 2 illustrates the selective FTIR spectra of (A) phen, (B) MS and (C) phen–Eu–MSMA. The spectrum of phen has a wide

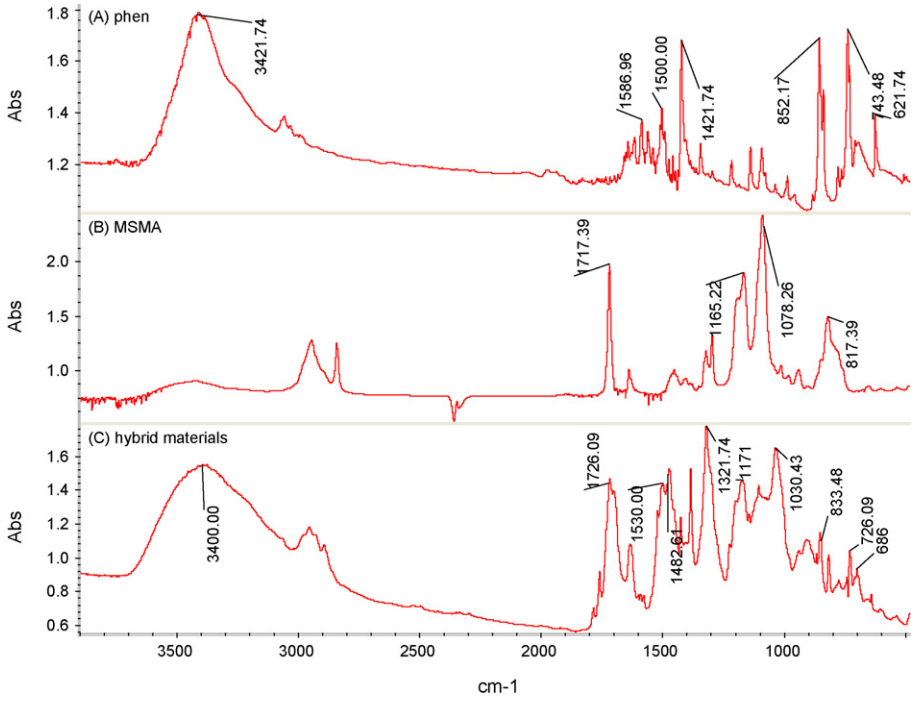

Fig. 2. FTIR spectra of (A) phen, (B) MSMA and (C) phen–Tb–MSMA.

band at 3200–3600 cm^{-1}, which is due to the hydroxyl group of crystal water in phen. This wide absorption band has become 3100–3700 cm^{-1} after the formation of hybrid materials for the hydrolysis/condensation reaction. The absorption peak at about 1587 cm^{-1} which is due to the stretching vibration of C=O in 1,10-phenanthroline shifted red to about 1530 cm^{-1}. The absorption peaks at about 852 and 743 cm^{-1} which are due to the bending vibration of C—H in 1,10-phenanthrole, also shifted red to about 833 and 726 cm^{-1}, respectively. The ν_{C-N} of 1,10-phenanthrole red shift from 1421 to 1392 cm^{-1}, a 29 cm^{-1} decrease. That is an indication of 1,10-phenanthroline and Eu^{3+} coordination bond formation, which is similar to the late reported earlier [33]. There exists an absorption peak at about 1717 cm^{-1} in the IR spectrum of MSMA, which is due to the acyl group. This peak still exists in the IR spectrum of the hybrid materials, but it shifted blue to about 1726 cm^{-1}. Therefore, the IR result confirmed the formation of ternary complex system in the hybrid materials. In contrast with the MS, no (Si—C) bond split happens in the spectra of hybrids, which are in harmony with the course of hydrolysis/condensation reactions. The similar feature can be found for the systems of Tb or Dy hybrids.

Fig. 3 exhibits representative ultraviolet absorption spectra of (A) phen/MSMA (the mixed of 1,10-phenanthroline and MSMA by the ratio of 2:1) and (B) phen–Eu–MSMA. From the spectra, it is observed that a blue shift (A → B) of the major π–π^* electronic transitions (from 237 to 220 nm) occurs and it is estimated that when the complex between Eu^{3+} and phen/MSMA formed the electron distribution of conjugated system has been modified. Therefore, we considered that 1,10-phenanthroline–MSMA has coordinated with Eu^{3+}, which also coincided with the result of IR spectra. Molecular phosphorescence belongs to the character of the organic molecular ligands and different phosphorescence bands correspond to different ligand molecules. The low temperature phosphorescence spectra of phen–Gd–MS at 77 K were measured owing to its high phosphorescence–fluorescence ratio compared to those of the other Ln^{3+} complexes and Gd^{3+} can sensitize the phosphorescence emission of ligands, which present the maximum peak at around 451 nm, similar to the phosphorescence spectrum of Gd–phen. This indicates that the phen behaves as the main energy donor in the ternary systems and it can be predicted the main sensitizer for the luminescence of rare earth ions in the resulting covalently bonded hybrid materials. The triplet state energy of phen can be determined to be 22,175 cm^{-1}, which is corresponded to the data from Refs. [34,35]. According to intramolecular energy transfer mechanism [36–40], the corresponding intramolecular transfer efficiency from the phen to RE^{3+} mainly depends on the energy match between the triplet state energy of phen and the resonant emissive energy level of the central RE^{3+} (17,300 cm^{-1} for Eu^{3+}, 20,500 cm^{-1} for Tb^{3+}, and 21,000 cm^{-1} for Dy^{3+}). The energy differences between the triplet state energy of phen and the resonant emissive energy level of Eu^{3+}, Tb^{3+}, and Dy^{3+} are 4875, 1675 and 1175 cm^{-1}, respectively. We can draw a conclusion that there exist good energy match between phen and Eu^{3+}, Tb^{3+} or Dy^{3+} ions. The effective luminescence for these hybrid materials can be predicted.

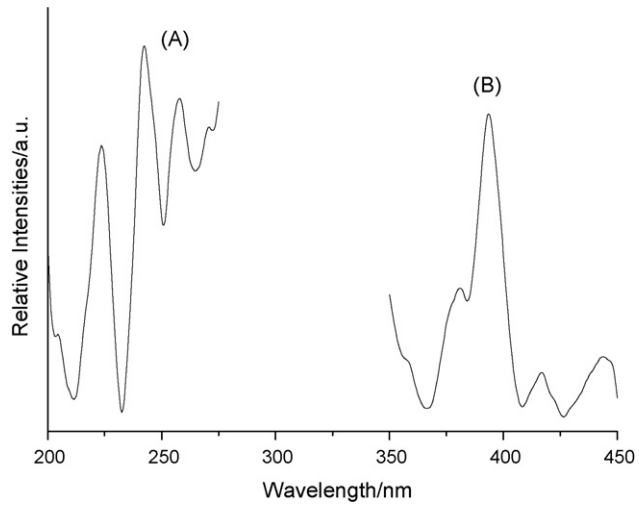

Fig. 4. Excitation spectra of phen–Eu–MSMA hybrid materials (A) short wavelength ultraviolet region and (B) long wavelength ultraviolet region.

The excitation spectra (Fig. 4) of phen–RE–MSMA obtained by monitoring the emission of Eu^{3+} ions at 615 nm and are dominated by a dominant broad band from 200 to 275 nm in short wavelength region and 325 to 450 nm in long wavelength region, respectively. The bands with maximum peak located at 225, 244, and 258 nm in short wavelength ultraviolet region are the characteristic absorption of the lanthanide complexes arising from the efficient transition based on the conjugated double bonds of the phen. Both these excitation spectra bands are the effective absorption for the luminescence of Eu^{3+}. Besides, there exists one weak absorption band of 393 nm in long wavelength ultraviolet

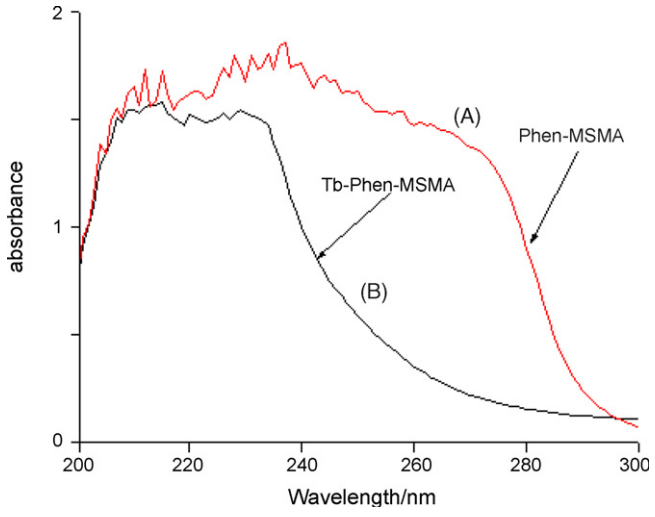

Fig. 3. Ultraviolet absorption spectra for (A) phen–MSMA and (B) phen–Tb–MSMA.

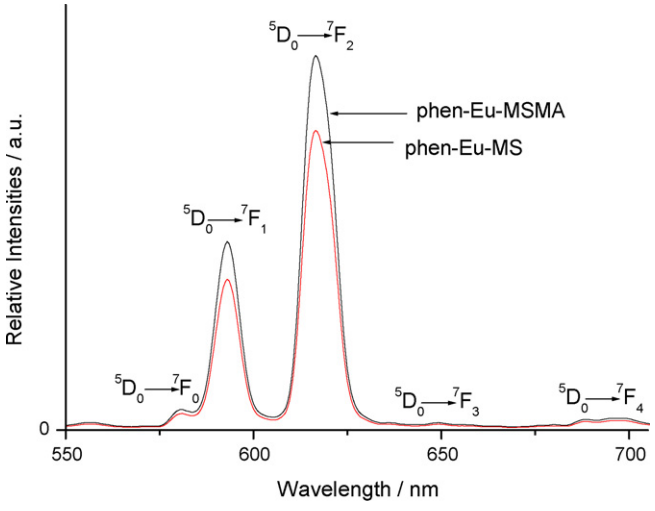

Fig. 5. Emission spectrum of phen–Eu–MSMA and phen–Eu–MS hybrid materials (λ_{ex} = 267 nm).

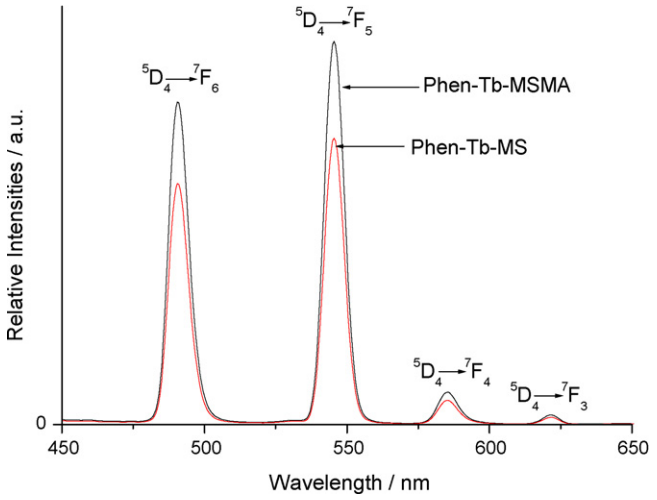

Fig. 6. Emission spectrum of phen–Tb–MSMA and phen–Tb–MS hybrid materials (λ_{ex} = 268 nm).

region, which belongs to the self-absorption of Eu^{3+} (f–f transition). The excitation spectra for phen–Tb–MSMA and phen–Tb–MS wear the similar features. The corresponding emission spectra for the ternary and quaternary hybrid materials were compared to study in Figs. 5–7. For europium hybrid materials, the emission spectra show five emission peaks under the excitation of 258 nm: 581, 593, 616, 649 and 698 nm, respectively, corresponded with the characteristic emission $^5D_0 \rightarrow {}^7F_J$ transitions (J = 0, 1, 2, 3, 4) of Eu^{3+} ion. Among the red luminescent intensity of $^5D_0 \rightarrow {}^7F_2$ transition is the strongest, and the emission intensity of $^5D_0 \rightarrow {}^7F_1$ transition becomes stronger, which maybe due to the surrounding environment of Eu^{3+} in the hybrid materials. For terbium hybrid materials, the emission spectra show four emission peaks under the excitation of 259 nm: 490, 545, 585 and 622 nm, attributed to be the characteristic emission $^5D_4 \rightarrow {}^7F_J$ (J = 6, 5, 4, 3) transition of Tb^{3+} ion. Among the $^5D_4 \rightarrow {}^7F_5$ transition exhibits the strongest green emission, and $^5D_4 \rightarrow {}^7F_6$ transition shows the second strongest blue emission. For dysprosium hybrid materials, the luminescence spectra show two apparent emission peaks under the excitation of 256 nm: one is at 483 nm, the other is at 574 nm, which corresponds to the characteristic emission $^4F_{9/2} \rightarrow {}^6H_J$ (J = 15/2, 13/2) transition of Dy^{3+} ion, respectively. And the blue emission possesses higher intensity than yellow one. These luminescence spectra indicate that the effective energy transfer take place between the aromatic ligand of 1,10-phenanthroline and the chelated RE^{3+} ions.

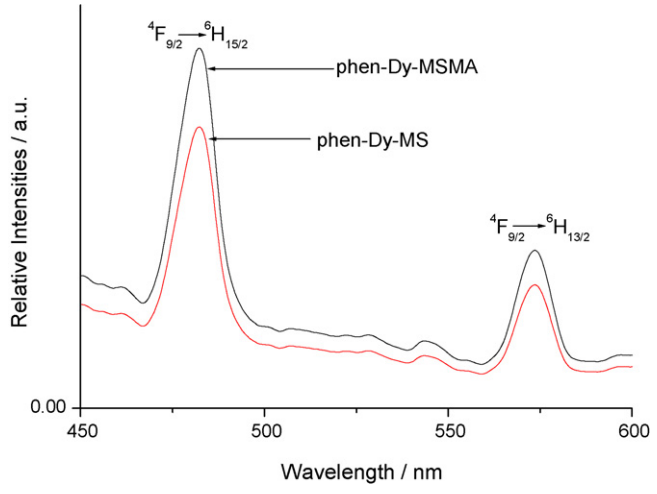

Fig. 7. Emission spectrum of phen–Dy–MSMA and phen–Dy–MS hybrid materials (λ_{ex} = 265 nm).

Further, we compared the luminescent intensities of the different rare earth hybrid materials, it can be seen that the europium hybrids present the higher intensities than those of terbium or dysprosium ones, which interpret that the triplet state energy of phen is more suitable for Eu^{3+} than Tb^{3+} or Dy^{3+} ions. The energy difference between triplet state energy of phen and the resonant emissive energy level of Tb^{3+} or Dy^{3+} ions are too small to cause inverse energy transition by thermal deactivation mechanism [39,40]. The luminescent phenomenon takes agreement from the prediction of energy match and energy transfer mechanism. Besides, it can also be observed that the quaternary hybrids with organic chain (MA) present slightly stronger luminescence than the ternary ones, suggesting the introduction of organic MA chain are beneficial for the luminescence of rare earth ions. And in both phen–RE–MS and phen–RE–MSMA hybrid systems, Eu^{3+} is the most suitable ion for the luminescence.

The typical decay curve of the Eu, Tb and Dy hybrid material were measured and they can be described as a single exponential ($\mathrm{Ln}(S(t)/S_0) = -k_1 t = -t/\tau$), indicating that all Eu^{3+}, Tb^{3+} and Dy^{3+} ions occupy the same average coordination environment. The resulting lifetimes of Eu and Tb, Dy hybrids were given in Tables 1 and 2, respectively. Quaternary hybrids phen–RE–MSMA exhibits the longer lifetime than ternary ones phen–RE–MS, indicating that the introduction of organic polymeric chain can enhance the luminescence stability of the whole hybrid systems. We further selectively determined the emission quantum efficiencies of the $^5D_0$ europium ion excited state for Eu^{3+} hybrids on the basis of the emission spectra and lifetimes of the $^5D_0$ emitting level using the four main equation according to Refs. [41–49]. The detailed principle and method was adopted as Ref. [42] and the data were shown in Table 1.

$$A_{0J} = A_{01}\left(\frac{I_{0J}}{I_{01}}\right)\left(\frac{\upsilon_{01}}{\upsilon_{0J}}\right) \quad (1)$$

$$A_{\mathrm{rad}} = \Sigma A_{0J} = A_{00} + A_{01} + A_{02} + A_{03} + A_{04} \quad (2)$$

$$\tau = {A_{\mathrm{rad}}}^{-1} + {A_{\mathrm{nrad}}}^{-1} \quad (3)$$

$$\eta = \frac{A_{\mathrm{rad}}}{A_{\mathrm{rad}} + A_{\mathrm{nrad}}} \quad (4)$$

Here A_{0J} is the experimental coefficient of spontaneous emissions, among A_{01} is the Einstein's coefficient of spontaneous emission between the $^5D_0$ and $^7F_1$ energy levels, which can be determined to be 50 s^{-1} approximately [46–49] and as a reference to calculate the value of other A_{0J}. I is the emission intensity and can be taken as the integrated intensity of the $^5D_0 \rightarrow {}^7F_J$ emission bands [42,43].

Table 1
The luminescent property data of europium molecular hybrids

Molecular hybrids	Phen–Eu–MSMA	Phen–Eu–MS
Emission band (nm)	581, 593, 616.5, 649, 698	580.5, 593, 616, 649, 698
Relative intensities (a.u.)[a]	5.80, 48.80, 99.70, 1.85, 3.10	4.65, 36.05, 79.60, 1.48, 2.58
Lifetimes (ms)[b]	0.51	0.42
Experimental decay rates (s^{-1})	1961	2381
Radiative decay rates (s^{-1})	167.83	177.47
Non-radiative decay rates (s^{-1})	1793.17	2303.53
Quantum efficiency (%)	8.56	7.45

[a] The relative intensities were obtained by the calculation of integral area of the same emission bands.
[b] For $^5D_0 \rightarrow {}^7F_2$ transition of Eu^{3+}.

Table 2
The luminescent property data of terbium and dysprosium molecular hybrids

Molecular hybrids	Phen–Tb–MSMA	Phen–Tb-MS	Phen-Dy-MSMA	Phen-Dy-MS
Emission band (nm)	490.5, 545.5, 585.5, 621.5	490, 545.5, 585.5, 622	482.5, 573.5	482.5, 574
Relative intensities (a.u.)[a]	69.41, 82.50, 6.77, 3.08	54.85, 61.65, 5.43, 2.75	33.49, 14.70	28.74, 13.88
Lifetimes (ms)[b]	0.62	0.55	0.49	0.42

[a] The relative intensities were obtained by the calculation of integral area of the same emission bands.
[b] For $^5D_4 \rightarrow {}^7F_5$ transition of Tb^{3+} and for $^4F_{9/2} \rightarrow {}^6F_{15/2}$ transition of Dy^{3+}.

υ_{0J} refers to the energy barrier and can be determined from the emission bands of Eu^{3+}'s $^5D_0 \rightarrow {}^7F_J$ emission transitions. A_{rad} and A_{nrad} mean to the radiative transition rate and non-radiative transition rate, respectively, among A_{rad} can be determined from the summation of A_{0J} (Eq. (2)). And then the luminescence quantum efficiency can be calculated from the luminescent lifetimes, radiative and non-radiative transition rates. Phen–MSMA–Eu polymeric hybrid material possesses the higher luminescence quantum efficiency than phen–Eu–MS hybrids. This takes agreement with the results from the luminescent intensities and lifetimes. The fabrication of organic polymer chain in the hybrid systems is favorable for the luminescent properties by increasing the ratio of radiative transition. The introduction of polymeric chain (MA) is beneficial to form the shielding environment for luminescent Eu ions in the whole covalently bonded hybrid matrix, while the pure Si—O network without MA chain can cause energy trap to decrease the energy transfer. But it can be seen the enhancement of luminescence quantum efficiency data are not so much as luminescent intensities, which is related with the absorption property of these hybrids.

Fig. 8 shows the representative scanning electron microscopy of phen–Eu–MS (A) and phen–Eu–MSMA (B), which indicates that there exists different microstructure influenced by the organic polymeric chain. Ternary hybrids phen–Eu–MS shows the simple porous structure with inorganic Si—O polymeric network, which arise from the sol–gel process because the chelation effect of europium ions and MS, phen cannot produce ordered orientation. While the quaternary hybrids phen–Eu–MSMA wears more regular layer microstructure. This can be interpreted that the organic polymer chain of MA form interpenetrating polymer network and have great influence on the polymeric tendency to determine the final micromorphology.

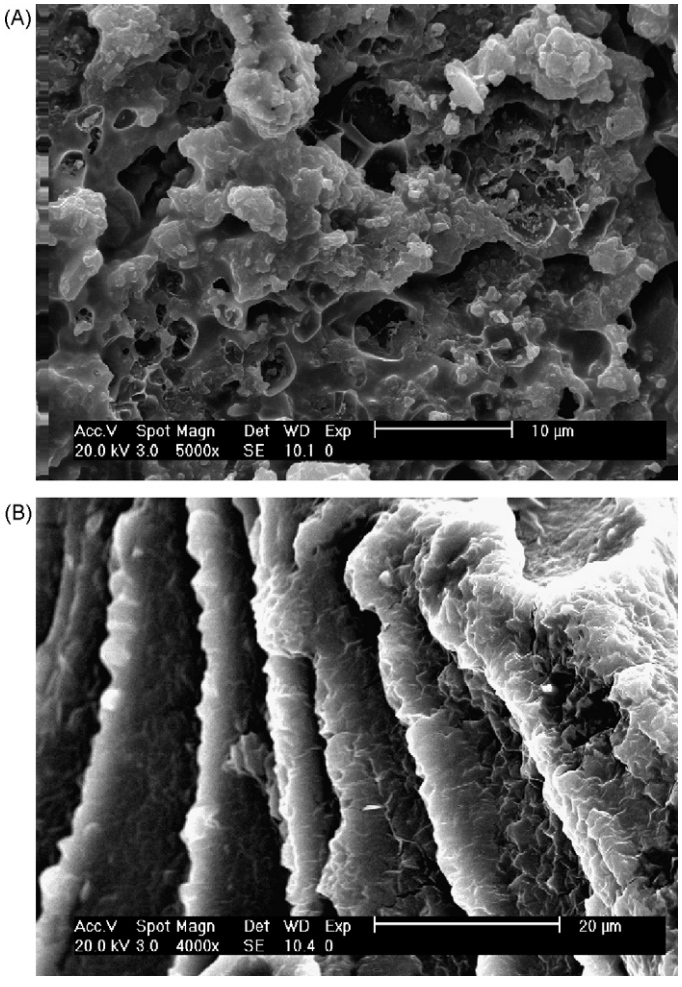

Fig. 8. SEM for the morphology of (A) phen–Eu–MS and (B) phen–Eu–MSMA hybrid materials.

5. Conclusions

Six novel kinds of rare earth/inorganic silica/organic polymer hybrid materials phen–RE–MSMA (MS) in which the organic component and inorganic component was connected through covalent bonds were constructed with MA, MS and rare earth complex systems of phen, which involves the long inorganic/organic hybrid polymeric chains through copolymerization and sol–gel process. Especially the photophysical properties of these quaternary hybrid materials were studied comparing with those of ternary hybrid materials phen–RE–MS. Correspondingly, it was worth pointing out that the quaternary hybrid materials (phen–Eu^{3+}(Tb^{3+}, Dy^{3+})–MSMA) with organic polymer unit present stronger luminescence intensities, longer lifetimes than those of ternary ones (phen–Eu^{3+}(Tb^{3+}, Dy^{3+})–MS), which is attributed to introduction of organic polymeric chain.

Acknowledgement

This work was supported by the National Natural Science Foundation of China (20301013, 20671072).

References

[1] E. Reichstein, Y. Shami, M. Ramjeesinch, E.P. Diamandis, Anal. Chem. 60 (1988) 1069–1074.
[2] Y.Y. Xu, I.A. Hemmilä, Anal. Chim. Acta 256 (1992) 9–16.
[3] L. Yan, Y.D. Yang, X.P. Ji, Chin. Anal. Chem. 20 (1992) 100–106.
[4] X.R. Liu, G. Xu, C.P. Richard, J. Solid State Chem. 62 (1986) 83–91.
[5] A.Y. Zhang, B. Qian, G.L. Gao, L.Y. Zhang, Chin. J. Inorg. Chem. 11 (1995) 168–173.
[6] L. Pasimeni, M. Meneghetti, R. Rella, L. Valli, C. Granito, L. Troisi, Thin Solid Films 265 (1995) 58–65.
[7] K.Z. Wang, C.H. Huang, G.X. Xu, X.S. Zhao, X.H. Xia, N.Z. Wu, L.G. Xu, X.K. Li, Thin Solid Films 252 (1994) 139–144.
[8] Z.B. Deng, J.G. Huang, S.Z. Deng, J.B. Wang, B. Zhang, F. Lu, H.H. Sun, J. Lumin. 17 (1996) 187–193.
[9] C. Guizard, P. Lacan, New J. Chem. 18 (1994) 1097–1104.
[10] U. Schubert, New J. Chem. 18 (1994) 1049–1057.
[11] J.I. Zink, J.S. Valentine, B. Dunn, New J. Chem. 18 (1994) 1109–1116.
[12] B.C. Dave, B. Dunn, J.S. Valentine, J.I. Zink, ACS Symp. Ser. 622 (1996) 351–356.
[13] E. Ruiz-Hitzky, P. Aranda, B. Casal, J.C. Galvan, Adv. Mater. 7 (1995) 180–184.

[14] M. Mennig, G. Jonschker, H. Schmidt, Institute for New Materials, German Patent DE 4 (1994) 217–222.
[15] P. Orgaz, H. Rawson, J. Non-Cryst. Solids 82 (1986) 57–64.
[16] C. Koeppen, S. Yamada, G. Jiang, A.F. Garito, L.R. Dalton, J. Opt. Soc. Am. B 14 (1997) 155–164.
[17] K. Kuriki, Y. Koike, Y. Okamoto, Chem. Rev. 102 (2002) 2347–2356.
[18] H. Liang, Q. Zhang, Z. Zheng, H. Ming, Z. Li, J. Xie, B. Chen, H. Zhao, Opt. Lett. 29 (2004) 1895–1898.
[19] B. Yan, H.J. Zhang, S.B. Wang, J.Z. Ni, Mater. Chem. Phys. 51 (1997) 92–96.
[20] Y. Okamoto, Macromolecules 14 (1981) 17–23.
[21] W.L. Li, T. Mishima, G. Adchi, J. Shiokawa, Inorg. Chim. Acta 121 (1986) 97–102.
[22] B. Vlasoula, P. Georgios, L. Panagiotis, Chem. Mater. 11 (1999) 3189–3195.
[23] H. Liang, B. Chen, Z.Q. Zheng, Phys. Status Solidi B 13 (2004) 3056–3062.
[24] Y.B. Lu, W.L. Sun, Z.Q. Shen, J. Appl. Polym. Sci. 96 (2005) 979–986.
[25] L. Delattre, C. Dupuy, F. Babonneau, J. Sol–Gel Sci. Technol. 2 (1994) 185–191.
[26] J.D. Miller, K.P. Hoh, H. Ishida, Polym. Compos. 5 (1984) 18–26.
[27] Q.M. Wang, B. Yan, J. Mater. Chem. 14 (2004) 2450–2455.
[28] Q.M. Wang, B. Yan, Cryst. Growth Des. 5 (2005) 497–503.
[29] Y.L. Sui, B. Yan, J. Photochem. Photobiol. A: Chem. 182 (2006) 1–6.
[30] V. Bekiari, G. Pistolis, P. Lianos, Chem. Mater. 11 (1999) 3189–3194.
[31] L.H. Wang, W. Wang, W.G. Zhang, E.T. Kang, W. Huang, Chem. Mater. 12 (2000) 2212–2218.
[32] Q.M. Wang, B. Yan, J. Photochem. Photobiol. A: Chem. 177 (2006) 1–5.
[33] L. Wang, J. Wu, Z. Zheng, C. Wei, G. Yamg, J. Lanzhou. Univ. 24 (1991) 50–54.
[34] Q.M. Wang, B. Yan, Inorg. Chem. Commun. 7 (2004) 1124–1127.
[35] Q.M. Wang, B. Yan, X.H. Zhang, J. Photochem. Photobiol. A: Chem. 174 (2005) 119–124.
[36] B. Yan, B. Zhou, J. Photochem. Photobiol. A: Chem. 171 (2005) 181–186.
[37] S. Sato, M. Wada, Bull. Chem. Soc. Jap. 43 (1970) 1955–1960.
[38] S.L. Wu, Y.L. Wu, Y.S. Yang, J. Alloy Compd. 180 (1994) 399–403.
[39] D.L. Dexter, J. Chem. Phys. 21 (1953) 836–841.
[40] T.D. Brown, T.M. Shepherd, J. Chem. Soc. Dalton Trans. (1973) 336–341.
[41] O.L. Malta, M.A. Couto dos Santos, L.C. Thompson, N.K. Ito, J. Lumin. 69 (1996) 77–84.
[42] O.L. Malta, H.F. Brito, J.F.S. Menezes, F.R. Goncalves e Silva, Alves, F.S. Farias, A.V.M. Andrade, J. Lumin. 75 (1997) 255–268.
[43] L.D. Carlos, Y. Messaddeq, H.F. Brito, R.A.S. Ferreira, V.D. Bermudez, S.J.L. Ribeiro, Adv. Mater. 12 (2000) 594–598.
[44] R.A.S. Ferreira, L.D. Carlos, R.R. Goncalves, S.J.L. Ribeiro, V.D. Bermudez, Chem. Mater. 13 (2001) 2991–2998.
[45] P.C.R. Soares-Santos, H.I.S. Nogueira, V. Felix, M.G.B. Drew, R.A.S. Ferreira, L.D. Carlos, T. Trindade, Chem. Mater. 15 (2003) 100–108.
[46] E.E.S. Teotonio, J.G.P. Espinola, H.F. Brito, O.L. Malta, S.F. Oliveria, D.L.A. de Foria, C.M.S. Izumi, Polyhedron 21 (2002) 1837–1844.
[47] S.J.L. Ribeiro, K. Dahmouche, C.A. Ribeiro, C.V. Santilli, S.H.J. Pulcinelli, J. Sol–Gel Sci. Technol. 13 (1998) 427–432.
[48] M.H.V. Werts, R.T.F. Jukes, J.W. Verhoeven, Phys. Chem. Chem. Phys. 4 (2002) 1542–1548.
[49] C.Y. Peng, H.J. Zhang, J.B. Yu, Q.G. Meng, L.S. Fu, H.R. Li, L.N. Sun, X.M. Guo, J. Phys. Chem. B 109 (2005) 15278–15287.